The cyclic antimicrobial peptide RTD-1 induces stabilized lipid–peptide domains more efficiently than its open-chain analogue

Peter M. Abuja[a], Alexandra Zenz[a], Manuela Trabi[b], David J. Craik[b], Karl Lohner[a,*]

[a]*Institute of Biophysics and X-Ray Structure Research, Austrian Academy of Sciences, Schmiedlstrasse 6, A-8042 Graz, Austria*
[b]*Institute for Molecular Bioscience, University of Queensland, Brisbane, Qld 4072, Australia*

Received 12 December 2003; revised 23 March 2004; accepted 30 March 2004

Available online 22 April 2004

Edited by Guido Tettamanti

Abstract The effects of a mammalian cyclic antimicrobial peptide, rhesus theta defensin 1 (RTD-1) and its open chain analogue (oRTD-1), on the phase behaviour and structure of model membrane systems (dipalmitoyl phosphatidylcholine, DPPC and dipalmitoyl phosphatidylglycerol, DPPG) were studied. The increased selectivity of RTD-1 for anionic DPPG over zwitterionic DPPC was shown by differential scanning calorimetry. RTD-1, at a molar peptide–lipid ratio of 1:100, induced considerable changes in the phase behaviour of DPPG, but not of DPPC. The main transition temperature, T_m, was unchanged, but additional phase transitions appeared above T_m. oRTD-1 induced similar effects. However, the effects were not observable below a peptide:lipid molar ratio of 1:50, which correlates with the weaker biological activity of oRTD-1. Small- and wide-angle X-ray scattering revealed for DPPG the appearance of additional structural features induced by RTD-1 above T_m, which were interpreted as correlated lamellar structures, with increased order of the fatty acyl side chains of the lipid. It is proposed that after initial electrostatic interaction of the cationic rim of the peptide with the anionic DPPG headgroups, leading to stabilized lipid–peptide clusters, the hydrophobic face of the peptide assists in its interaction with the fatty acyl side chains eventually leading to membrane disruption.

Keywords: RTD-1; Rhesus theta defensin; Model membranes; Antimicrobial peptides; Defensin; DSC; Small-angle X-ray scattering

1. Introduction

Mammalian defensins play an important role in innate immunity [1] and like other antimicrobial peptides they may serve in future as substitutes for conventional antibiotics, a prospect which becomes increasingly important considering the growing problems associated with microbial resistance against antibiotics [2].

One conceivable mechanism of action of such antimicrobial peptides is the perturbation of the integrity of bacterial membranes, eventually leading to loss of plasma membrane function, e.g. by lysis [3]. Two general mechanisms have been discussed, the barrel-stave mechanism in which the peptides integrate into the membrane to form a toroidal pore [4] and the carpet mechanism, in which peptides assemble at the headgroup region of the bilayer and act in a detergent-like fashion to disrupt the membrane [5]. These are probably not the only feasible mechanisms. Others include the induction of lipid unmixing, which will eventually lead to defunctionalization of the membrane, or the formation of non-bilayer structures, such as cubic phases [6]. Penetration of the bilayer and some direct action upon binding of an intracellular target have also been discussed [7,8].

Over the years it has turned out that an important issue with respect to the usability of peptide antibiotics is that they should exhibit high selectivity for (negatively charged) bacterial membranes, to avoid toxicity against mammalian cells, while preserving efficient bactericidal properties. Many natural antimicrobial peptides are therefore cationic, and their mechanism of action is presumed to involve initial binding due to electrostatic interaction, followed by perturbation of the normal phase behaviour of the plasma membrane [9]. As biological membranes are apparently designed to be in a state close to a phase transition at the environmental conditions the organism normally encounters [10–12], even slight shifts in phase behaviour may impart membrane properties such as to seriously affect cell viability.

Considering the wide variety of peptides exhibiting antimicrobial properties, no consensus mechanism can be expected. Moreover, in most cases the mode of action on bacterial membranes is largely unknown.

Defensins are small cysteine-rich antimicrobial peptides. The α- and β-defensins are the predominant defensin subfamilies, which are also expressed in primates and humans. The θ-defensins, which have been found in rhesus macaque leukocytes [13], are unusual as they have a circularized peptide chain derived from two precursor defensins, which themselves show high sequence homology to α-defensins. The two strands of their antiparallel β-sheet are linked by three disulfide bonds to give a boat-like structure with a charged face and a hydrophobic face that exposes the cystine side chains [14].

* Corresponding author. Fax: +43-316-4120-390.
E-mail address: karl.lohner@oeaw.ac.at (K. Lohner).

Abbreviations: RTD-1, rhesus theta defensin 1; oRTD-1, open chain form of RTD-1; DPPC, dipalmitoyl-*sn*-glycero-3-phosphocholine; DPPG, dipalmitoyl-*sn*-glycero-3-[phospho-*rac*-(l-glycerol)] (Na-salt); DSC, differential scanning calorimetry; PBS, phosphate buffered saline; SAXS, small-angle X-ray scattering; WAXS, wide-angle X-ray scattering

0014-5793/$22.00 © 2004 Federation of European Biochemical Societies. Published by Elsevier B.V. All rights reserved.
doi:10.1016/j.febslet.2004.03.112

Here we report the effects of such a cyclic antimicrobial peptide, rhesus theta defensin 1 (RTD-1) (Sequence GFCRCLCRRGVCRCICTR), and its open chain analogue (oRTD-1) [13], on the phase behaviour of two membrane mimetic systems, i.e., liposomes consisting of dipalmitoylphosphatidylcholine (DPPC; dipalmitoyl-*sn*-glycero-3-phosphocholine) and dipalmitoyl-phosphatidylglycerol (DPPG; dipalmitoyl-*sn*-glycero-3-[phospho-*rac*-(l-glycerol)] (Na-salt)), representative lipids for mammalian and bacterial plasma membranes, respectively.

2. Materials and methods

Phospholipids, DPPC and DPPG, were obtained from Avanti Polar Lipids (Alabaster, AL, USA) and used without further purification (>99%). All other chemicals were of analytical grade and from Sigma or Merck (both Vienna, Austria). Before and after calorimetric and X-ray measurements, the purity of both phospholipids was checked by thin layer chromatography to exclude degradation. $CHCl_3/CH_3OH/NH_{3,conc}$ (75:25:6, v:v:v) was used as a solvent and aluminium sheets, silica gel 60, purchased from Merck (Darmstadt, Germany), were used as stationary phase.

2.1. Synthesis of RTD-1 and oRTD-1

RTD-1 and oRTD-1 were synthesized using BOC chemistry [15]. Formation of the disulfide bonds was achieved by air oxidation overnight. For RTD-1, the oxidized peptide was cyclized as described in [14]. Purity was confirmed by HPLC and mass spectrometric analysis.

2.2. Preparation of multilamellar and unilamellar liposomes

Lipids were dissolved in chloroform and deposited as a film on the inside of a test tube by evaporation under a stream of nitrogen. After drying overnight in vacuum, the films were suspended in phosphate buffered saline (PBS, 20 mM Na-phosphate, 130 mM NaCl, pH = 7.4) and hydrated under intermittent vortexing over 4 h at 50 °C for DPPC, or incubated at 65 °C and vortexed at 5,10, 20, 30, 60 and 90 min for 1 min for DPPG (this procedure yields large unilamellar liposomes) [16]. Peptides were added at the appropriate concentrations to the hydrating buffer.

2.3. Differential scanning calorimetry

Differential scanning calorimetry (DSC) experiments were performed in a Microcal VP-DSC scanning microcalorimeter (Northampton, MA, USA), at a lipid concentration of 1 mg/ml in PBS. Peptides were present at the indicated molar peptide:lipid ratios. Heating and cooling scans were performed between 20 and 50 °C for DPPC and 10–60 °C for DPPG, at a scan rate of 30 °C/h and prescan thermal equilibration of 10 and 20 min, respectively.

2.4. Small-angle and wide-angle X-ray scattering

Small-angle and wide-angle X-ray scattering (SAXS, WAXS) experiments were performed on a modified Kratky compact camera (SWAX, Hecus X-ray Systems, Graz, Austria) allowing simultaneous recording of diffraction data in the small-angle and wide-angle region [17]. Ni-filtered CuK_α-radiation was used ($\lambda = 1.542$ Å) at 4 kW power, originating from a rotating-anode X-ray generator (Rigaku-Denki, Japan). The camera was equipped with a Peltier-controlled thermostatted sample stage (temperature resolution 0.1 °C) and two linear position-sensitive detectors. Angular calibration in the small-angle region was obtained using silver stearate, in the wide-angle region *p*-Br benzoic acid was used. Temperature control and data acquisition were achieved by a programmable temperature and time controller (MTC 2.0, Hecus X-Ray Systems, Graz, Austria). After equilibration of the samples to the respective temperature for 1000 s (2000 s for downscans), data were recorded for 9000 s at each temperature, allowing for 7200 s in the small-angle region and 1800 s in the wide-angle region.

3. Results

3.1. Selectivity of RTD peptides towards zwitterionic (DPPC) and anionic (DPPG) lipids

In zwitterionic DPPC liposomes, both RTD-1 and oRTD-1 at a peptide:lipid molar ratio of 1:25 had minimal effect on the chain melting or main transition temperature T_m (for DPPC the temperature of the transition between lamellar gel, $P_{\beta'}$, and liquid crystalline phase, L_α) at around 41 °C (Fig. 1A). A slight increase was observed in the temperature of the pretransition (lamellar tilted gel, $L_{\beta'}$, to the ripple phase, $P_{\beta'}$) at about 34 °C, for RTD-1, indicating a slight stabilization of the $L_{\beta'}$ over the

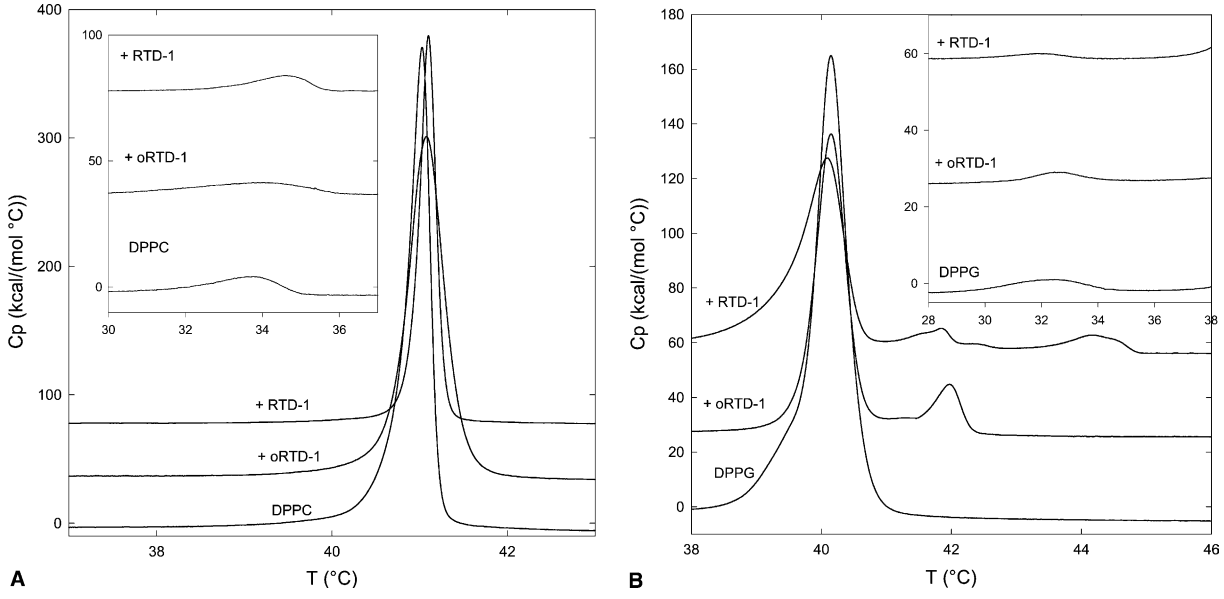

Fig. 1. Excess heat capacity function of the interaction of RTD-1 and oRTD-1 with (A) DPPC and (B) DPPG at a peptide:lipid molar ratio of 1:25 (heating scans), in PBS. For clarity, the curves have been separated by incrementing Cp. The insets show the pretransition part of the thermograms, the main graphs the main transition part.

$P_{\beta'}$ phase, while oRTD-1 strongly decreased the cooperativity (indicated by the increase in half-width) of the pretransition, resulting in a very flat wide peak.

Interaction of the peptides with anionic DPPG resulted in significant changes (Fig. 1B). Although T_m again remained unchanged within experimental error at around 40 °C, two additional thermotropic phase transitions were observed for oRTD-1, at about 41–42 °C, and up to five for RTD-1, in the range between 41 and 45 °C. The enthalpy of the main transition was reduced in the presence of peptide, however, post-main transition enthalpies make up for the difference. This indicates that all lipid molecules eventually melt, including those engaged in interaction with peptide. Pretransition temperatures did not vary appreciably, and cooperativity was notably decreased for RTD-1, and less pronouncedly for oRTD-1.

It should be noted that the cooling scans did not show transitions above T_m, most likely due to kinetic hindrance of subdomain formation. However, there were weak additional transitions observable below T_m (Fig. 2C), for the peptide:lipid molar ratio of 1:25 the additional transitions have merged with the main transition peak, leading to a widening of this peak.

3.2. Sensitivity of DPPG model membranes towards RTD-1 and oRTD-1

To investigate the molecular reason for the reported different antibacterial activity we checked the sensitivity of DPPG towards RTD-1 and oRTD-1 by using the peptides at different peptide:lipid molar ratios. RTD-1 still showed a notable additional transition above T_m at a peptide:lipid molar ratio of 1:100, at around 42 °C (Fig. 2A); when induced by oRTD-1, this transition vanished at peptide:lipid molar ratios above 1:50. Also, for both peptides, ΔH_m decreased with increasing peptide concentrations, which is indicative of lipids associating with peptides, resulting in the inability of the lipids to participate in the main transition and to contribute to the melting enthalpy.

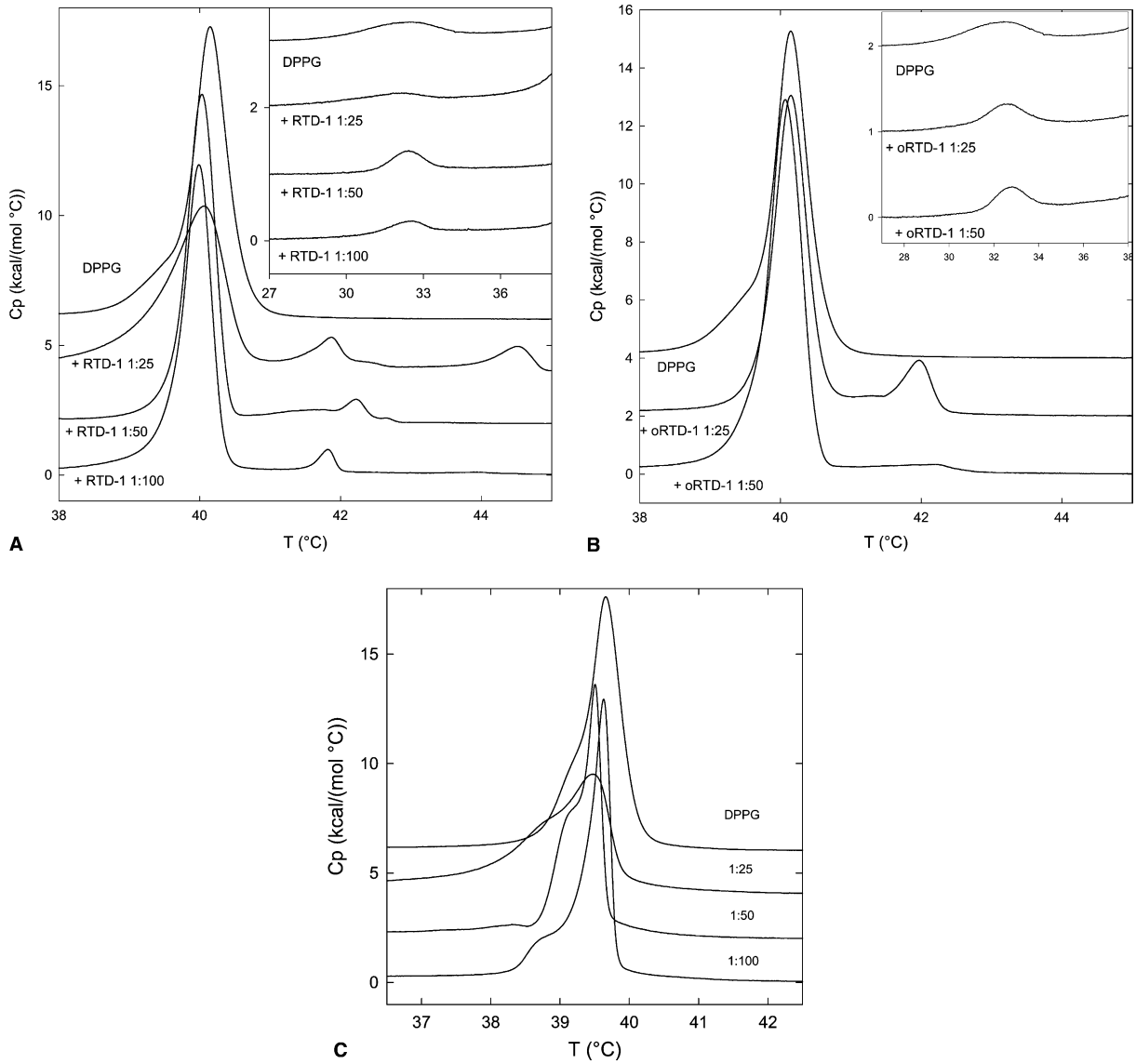

Fig. 2. Excess heat capacity function of DPPG with (A) RTD-1 at peptide:lipid molar ratios of 1:25, 1:50 and 1:100. (B) oRTD-1 at 1:25 and 1:50 (heating scans), in PBS. For clarity the curves have been displaced by incrementing Cp. The insets show the pretransition region of the thermograms, the main graphs the main transition region. (C) Cooling scans of RTD-1 as in panel A (data smoothed for clarity).

3.3. SAXS and WAXS measurements of RTD-1 and oRTD-1 in DPPG liposomes

To find out more about the mechanism of the interaction of RTD-1 with DPPG we studied the structural effects of the peptides on DPPG liposomes. At NaCl concentrations of up to 150 mM, DPPG forms large unilamellar vesicles after preparation according to the protocol given in 2.1 [16]. Indeed, at 20 °C such vesicles could also be observed in the presence of RTD-1 (peptide:lipid molar ratio of 1:25), characterized by diffuse scattering which exhibited a rather broad side maximum at $q = 0.105$ Å^{-1} (Fig. 3A). Wide-angle scattering data showed abroad reflection around $q = 1.5$ Å^{-1} (Fig. 3B) indicative of local order in the packing of the DPPG hydrocarbon chains. With increasing temperature the smooth shape of the side maximum (SAXS) became partially superimposed by two (first order) Bragg reflections at $q = 0.0927$ Å^{-1} ($d = 67.8$ Å) and 0.127 Å^{-1} ($d = 49.5$ Å), respectively, which were most pronounced at $T = 43$ °C and disappeared again when the sample was heated to $T = 50$ °C. Additional weak peaks became visible at $q = 0.251$ Å^{-1} ($d = 25.0$ Å) and 0.382 Å^{-1} ($d = 16.4$ Å), which are the second order reflections (not shown). Concomitantly, the wide-angle peak at around $d = 1.50$ Å^{-1} ($d = 4.20$ Å) became sharper with the appearance of the SAXS Bragg reflections, indicating increased packing order of the DPPG hydrocarbon chains, and disappeared only at $T = 50$ °C, while pure DPPG showed this peak only below 40 °C (not shown). Upon cooling, the Bragg reflections did not reappear, consistent with the observations by DSC. The SAXS scattering is consistent with the formation of mixed lamellar phases, which is also corroborated by the appearance of WAXS reflections.

For oRTD-1, similar effects were found (Fig. 3C and D), however, the wide-angle reflection at 1.50 Å^{-1} is much weaker, indicating less efficient chain-packing. This peak completely disappears above 41 °C, corresponding to the disappearance of the weak SAXS Bragg reflection above 41 °C. Interestingly, at 50 °C a new SAXS Bragg peak at 0.105 Å^{-1} ($d = 59.8$ Å) appears, indicating a new correlated lamellar fluid phase (evident by the lack of a wide-angle reflection).

4. Discussion

Investigation of the influence of RTD-1 and oRTD-1 on the phase behaviour of zwitterionic DPPC and anionic DPPG liposomes corroborated the reported selectivity for (negatively charged) bacterial membranes. The peptides were not able to notably alter the phase transition properties of DPPC. However, in DPPG the peptides, in particular RTD-1, induced the formation of additional phases. A possible explanation for the observed phase transitions at temperatures above T_m is that lipids engage with the peptides in the formation of small domains that are stabilized by electrostatic and hydrophobic interactions. The phase separation induced by this process can be the trigger for loss of membrane integrity, and thus explain the bactericidal activity of the peptides. This is corroborated

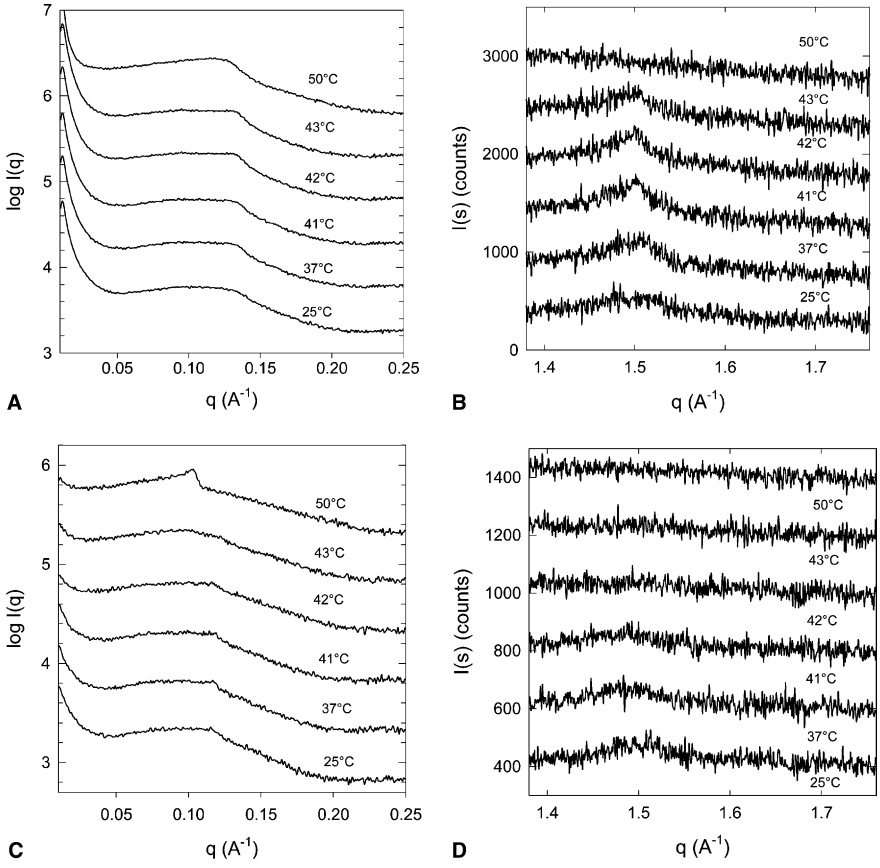

Fig. 3. SAXS (A,C) and WAXS (B,D) diffractograms of DPPG, in the presence of RTD-1 (A,B) and in the presence of oRTD-1 (C,D) at a peptide:lipid ratio of 1:25. Scattering intensity is plotted versus q ($q = 4\pi/\lambda \sin\theta$; magnitude of the scattering vector).

by the finding of kinetically stabilized domains during the DSC downscans, which 'freeze' below T_m (Fig. 2C).

SAXS diffraction parallels the DSC results, as at temperatures above the main transition additional structural features appear, which may be interpreted as correlated lamellar structures induced by the peptide. The lipid ordering effect at $T > T_m$ is also reflected in increased side chain ordering observed in the wide-angle pattern in the presence of RTD-1, which corroborates this notion. The appearance of a SAXS Bragg peak at 50 °C in presence of oRTD-1, corresponding to a correlated, fluid lamellar phase, is probably a consequence of the additional charge at the open ring ends of oRTD-1, which aids in shielding the charges of DPPG, thus permitting correlation of the bilayers. The superiority of RTD-1 over oRTD-1 in its bactericidal activity was reflected by the observation that RTD-1 was able to induce this phase separation at concentrations which were only half of those of oRTD-1 required to have the same effect. Moreover, the observation that oRTD-1 leads to less efficient hydrocarbon chain packing as evident from WAXS reflections (Fig. 3D) than RTD-1 (Fig. 3B), which completely disappear above 41 °C, confirms the reduced ability of oRTD-1 to form stabilized domains.

With its unique circular peptide backbone and three disulfide bonds, RTD-1 exhibits a structure that is novel among antimicrobial peptides. Recent NMR studies [14] showed that despite the conformational restrictions imposed by its head-to-tail cyclized backbone and the laddered disulfide bonds RTD-1 exhibits a specific type of internal flexibility. In particular, the turns on both ends of the elongated β-sheet region are very well defined but are involved in a hinge-like motion with respect to the β-sheet part of the molecule [14].

Many open chain peptides display a random structure in solution and only adopt the secondary structure of the active form upon interaction with the membrane. One prominent example of this behaviour is PGLa [18], a 21-residue cationic peptide from the skin of the South African frog *Xenopus laevis*. In contrast, RTD-1 is expected to show a similar structure both in solution and in contact with membranes, due to the structural restriction mentioned above. However, the mobility of the molecule may assist in directing the positively charged arginine side chains, which, in aqueous solution, are almost evenly distributed over the surface of RTD-1 (Fig. 4), towards one face of the molecule, while exposing the disulfide bonds and hydrophobic side-chains on the other face. It is therefore conceivable that the positively charged Arg side chains initially interact with the negatively charged DPPG headgroups, resulting in stabilized lipid–peptide clusters. This proposal is consistent with recent findings by Weiss et al. [19], who noted that RTD-1 shows two physically distinct bound states in lipid bilayers. In one state RTD-1 is oriented with its backbone ring parallel to the bilayer plane, corresponding to the initial stage of electrostatic interaction described above. The second state could not be fully defined by Weiss et al., but it seems to be different from both the initial and the so-called I state known from other antimicrobial peptides [19]. It seems likely that the hydrophobic face of the peptide would interact with the hydrocarbon chains of the phospholipid, which may eventually lead to voids in the hydrophobic core and consequential membrane disruption.

Although the exact mode of interaction and the nature of the antimicrobial activity of RTD-1 is still unknown it is interesting to note that the positive charges in RTD-1 are associated with Arg residues rather than Lys residues. Arg residues contain a substantially hydrophobic side chain and on average score more highly on hydrophobicity scales than Lys residues [20].

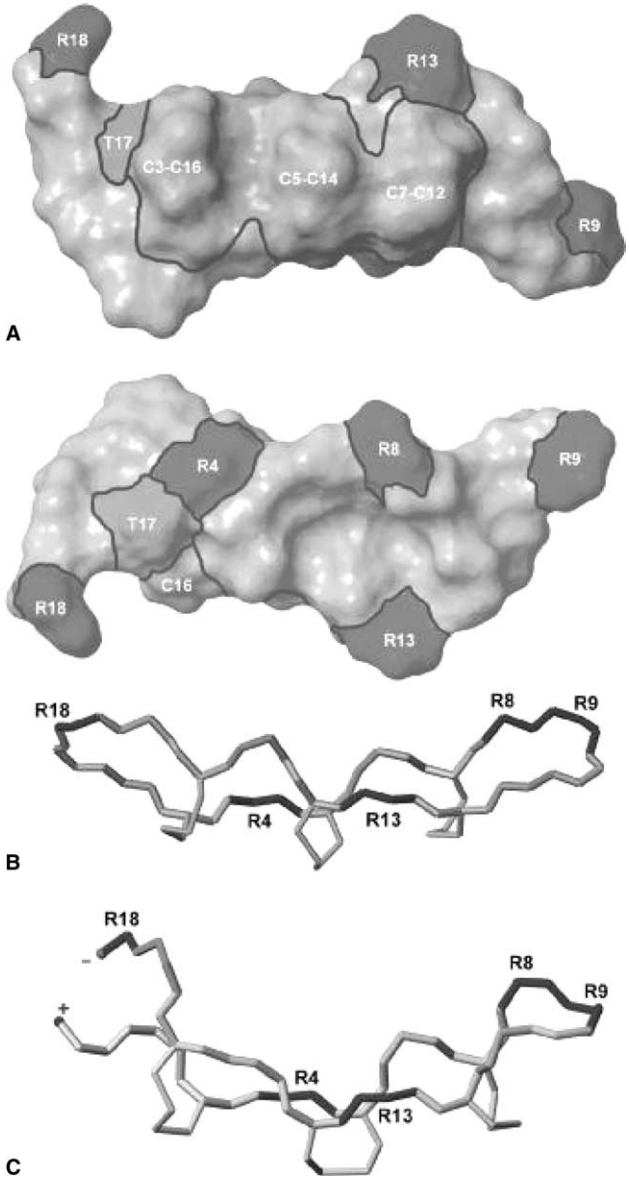

Fig. 4. (A) Surface representations of RTD-1 showing the distribution of positive (dark grey), polar (T17), hydrophobic (light grey) and cysteine residues (medium grey) for a typical structure from the ensemble of NMR-derived structures. Note that the family of NMR structures of RTD-1 suggests a degree of flexibility characterized by bending motions about the plane containing the elongated cyclic backbone, but also slight torsion. Individual structures show variability in the precise positioning of the amino acid side chains, but the trend of one charged face and one face dominated by the disulfide bonds is common to all structures. The two surface representations are rotated 180° with respect to one another. (B,C) Models of RTD-1 (B) and oRTD-1 (C) showing the peptide backbone and the disulfide bonds. The terminal charges in oRTD-1 are indicated by + and −, the residues are coloured as in A.

NMR studies have shown that RTD-1 and oRTD-1 have similar solution structures as well as a comparable degree of flexibility [14]. Therefore, the reduced biological activity of oRTD-1 may reflect the charge re-distribution created by the

introduction of a negative charge at the C-terminus, rather than a structural or motional difference between the two peptides – the charged C-terminus might, for instance, reduce the membrane insertion of oRTD-1.

In summary we have demonstrated that both RTD-1 and oRTD-1 show high selectivity for anionic DPPG over zwitterionic DPPC. In spite of the identical amino acid sequence and of the very similar tertiary structure, the activity of RTD-1 towards DPPG is significantly higher. This illustrates one of the inherent difficulties of understanding the mechanism of antimicrobial peptide action: apparently minimal differences may have significant consequences.

Acknowledgements: This study has been carried out with financial support from the Commission of the European Communities, specific RTD programme "Quality of Life and Management of Living Resources", QLK2-CT-2002-01001, "Antimicrobial endotoxin neutralizing peptides to combat infectious diseases".

References

[1] Hancock, R. and Scott, M. (2000) Proc. Natl. Acad. Sci. USA 97, 8856–8861.
[2] Lohner, K. and Staudegger, E. (2001) Are we on the threshold of the post-antibiotic area? in: Development of novel antimicrobial agents: emerging strategies (Lohner, K., Ed.), pp. 1–15, Horizon Scientific Press, Wymondham, UK.
[3] Epand, R. and Vogel, H. (1999) Biochim. Biophys. Acta 1462, 11–28.
[4] Matsuzaki, K. (1999) Biochim. Biophys. Acta 1462, 1–10.
[5] Shai, Y. (1995) Trends Biol. Sci. 20, 460–465.
[6] Staudegger, E., Prenner, E.J., Kriechbaum, M., Degovics, G., Lewis, R.N.A.H., McElhaney, R.N. and Lohner, K. (2000) Biochim. Biophys. Acta 1468, 213–230.
[7] Park, C.B., Kim, H.S. and Kim, S.C. (1998) Biochem. Biophys. Res. Commun. 244, 253.
[8] Wu, M., Maier, E., Benz, R. and Hancock, R.E.W. (1999) Biochemistry 38, 7235–7242.
[9] Lohner, K. (2001) The role of membrane lipid composition in cell targeting of antimicrobial peptides. in: Development of novel antimicrobial agents: emerging strategies (Lohner, K., Ed.), pp. 149–165, Horizon Scientific Press, Wymondham, UK.
[10] Gruner, S.M. (1992) Non-lamellar lipid phases. in: Structure of biological membranes (Yeagle, P.L., Ed.), pp. 211–250, CRC Press, Boca Raton, FL.
[11] Morein, S., Andersson, A.S., Rilfors, L. and Lindblom, G. (1996) J. Biol. Chem. 271, 6801–6809.
[12] Foht, P.J., Tran, Q.M., Lewis, R.N.A.H. and McElhaney, R.N. (1995) Biochemistry 34, 13811–13817.
[13] Tang, Y.-Q., Yuan, J., Österbay, G., Österbay, K., Tran, D., Miller, C.J., Ouellette, A.J. and Selsted, M.E. (1999) Science 268, 498–502.
[14] Trabi, M., Schirra, H.J. and Craik, D.J. (2001) Biochemistry 40, 4211–4221.
[15] Schnölzer, M., Alewood, P., Jones, A., Alewood, D. and Kent, S.B.H. (1992) Int. J. Peptide Protein Res. 40, 180–193.
[16] Degovics, G., Latal, A. and Lohner, K. (2000) J. Appl. Cryst. 33, 544–547.
[17] Laggner, P. and Mio, H. (1992) Nucl. Instr. Meth. Phys. Res. A 323, 86–90.
[18] Latal, A., Degovics, G., Epand, R.F., Epand, R.M. and Lohner, K. (1997) Eur. J. Biochem. 248, 938–946.
[19] Weiss, T.M., Yang, L., Ding, L., Waring, A.J., Lehrer, R.I. and Huang, H.W. (2002) Biochemistry 41, 10070–10076.
[20] Trinquier, G. and Sanejouand, Y.-H. (1998) Protein Eng. 11, 153–169.